

# Influence of configuration and acoustic phonons on three-qubit controlled-phase gate

Song Yang, Ming Gong, Xubo Zou\*, Chuanfeng Li, Cheng Zhao, and Guangcan Guo

*Key Laboratory of Quantum Information,  
University of Science and Technology of China,  
Hefei, 230026, People's Republic of China*

(Dated: November 6, 2018)

## Abstract

We discuss the configuration and acoustic phonon effect on the conditional phase gate using self assembled quantum dots. As an example, we discuss the simplest three dots conditional phase gate, and we found that the fidelity of conditional phase gate depends strongly on the configuration and temperature. Numerical simulation shows that line-configuration resonant with lower single exciton energy level performs better during the gate operation.

---

\* xbz@ustc.edu.cn

The implementation of a sequence of quantum gate operations and the ability to initialize the qubits are prerequisites for quantum information processing (QIP). So far, the two-qubit controlled-NOT (CNOT) and controlled PHASE (CPHASE) gates have been demonstrated experimentally in cavity[1], ion traps[2], NMR[3], quantum dot (QD)[4] and superconductor system[5], and the three-qubit CPHASE gate in NMR system has also been reported recently[6]. However, among all the realization schemes, the electron spin in QD attracts special interest due to the integrated advantages: (i), the spin in QD can be manipulated ultrafast by a circularly polarized pulse ( $\sim$  ps), which may be more readily realized with current technology. (ii), the QDs can be scaled up to large network benefitted from the state-of-the-art electronics. (iii), the spin decoherence lifetime is very long[7, 8], so numerous operations can be performed before the coherence is totally lost during the interaction between QDs and the phonon bath.

Recently, a scheme to realize CPHASE gate using QD molecular has been proposed by Gauger *et al*[9, 10], who shows that the phonon bath has huge influence on the CPHASE. Here, we extend this model to three QDs system, which is of great importance in QIP. In this letter, we focus on the configuration effect on the CPHASE operation.

The system we studied is composed of three lateral coupled QDs, as schematically shown in Fig. 1, (a) is ring configuration and (b) is the line configuration. We use electron spins to realize the CPHASE because the spin has sufficiently long decoherence time [11]. In self-assembled QDs, the lattice mismatch between the QD and the substrate break the degenerate of heavy hole (HH) and light hole (LH) by about 200 meV, hence the HH can be well described by  $\pm\frac{3}{2}$ . The tunneling effect decreases quickly as the distance between dots increases, and can be neglected. The hamiltonian to describe this system hence read as

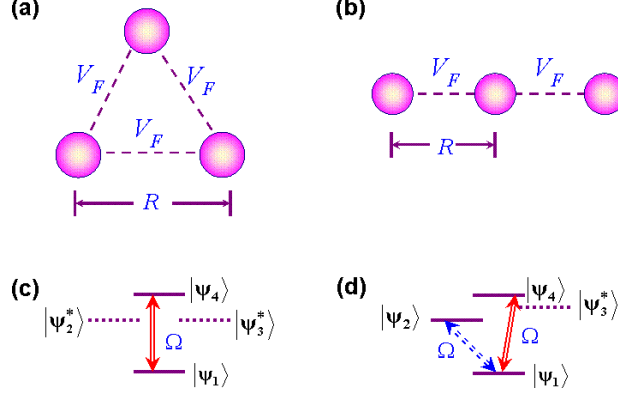


FIG. 1: (color online). Possible configuration of three quantum dots, ring for (a) and line for (b). We assume that the three quantum dots have identical exciton energy and have the same exciton transfer rate. Due to Förster interaction between the coupled QDs, energy shift on single-exciton states in subspace  $\mathcal{H}$  occurs. We can choose an appropriate single-exciton state as auxiliary state to achieve CPHASE gate. The energy level diagrams of ring and line configuration are shown in (c) and (d) respectively. The arrows denote the possible resonant transitions to implement gate operation: only  $|\Psi_1\rangle \leftrightarrow |\Psi_4\rangle$  is allowed in ring structure, both  $|\Psi_1\rangle \leftrightarrow |\Psi_2\rangle$  and  $|\Psi_1\rangle \leftrightarrow |\Psi_4\rangle$  are possible in line structure.

$$H_0 = \omega_a \sum_i n_i + V_F \sum_{\langle i,j \rangle} c_i^\dagger c_j + V_{xx} \sum_{\langle i,j \rangle} n_i n_j, \quad (1)$$

where  $c_i$  and  $c_i^+$  is the destruction and creation operator of exciton at the  $i^{\text{th}}$  QD.  $V_F$  is the Förster energy transfer rate between coupled QDs. It is dominated by the dipole-dipole interactions, and has recently been demonstrated by Kim *et al* in semiconductor QDs[12]. The third term  $V_{xx}$  is the Coulomb interaction between the coupled QDs, and may contribute to the system when each QD contains one exciton.

We now impose a time-dependent and  $\sigma^+$  polarized laser pulse to realize the three QDs

CPHASE gate. The Hamiltonian can be written as

$$H_i = \Omega \cos(\omega_l t) \sum_i (c_i^\dagger + c_i) \quad (2)$$

where  $\omega_l$  is the frequency of the external field, and  $\Omega$  is the corresponding coupling constant. Because the external field is  $\sigma^+$  polarized, so only  $|X_{\uparrow}^+\rangle = |\uparrow\downarrow\rangle$  is possible to be created when the qubit is initialized to  $|\uparrow\rangle$ [13]. If the qubit is initialized at  $|\downarrow\rangle$ , no exciton will be created in the QDs because of the Pauli blocking effect. With the above restriction, the hamiltonian can be decoupled into four subspaces sorted by the number of qubit in the basis state  $|\uparrow\rangle$ . Additionally, with the help of Förster interaction  $V_F$  and Coulomb interaction  $V_{xx}$ , the energy shifts lifted in each subspace are different. We are primed to pay attention to the subspace  $\mathcal{H}$  with its electron state  $|\uparrow\uparrow\uparrow\rangle$ , whose level schemes as shown in Fig. 1 (c) (ring configuration) and Fig. 1 (d) (line configuration).

*One-step CPHASE gate.*—Most three-qubit phase gate requires a lot of two-qubit gates and one-qubit rotations[14], or performing many steps by addressing individual qubit with laser pulses[15]. In this work, the CPHASE gate can be realized in only one step. First, we will study the performance of the CPHASE gate in the ideal case without any dephasing mechanism. We derive Eq.(1) into the subspace  $\mathcal{H}$  with its eight eigenvectors. We drive the system with a  $\sigma^+$  laser field tuned on resonance with the transition  $|\uparrow\uparrow\uparrow\rangle \leftrightarrow |\Psi_s\rangle$ , and  $|\Psi_s\rangle$  is an auxiliary state. Assuming other off-resonant transitions are so far off the resonance that no transition is induced through it, we can get an effective Hamiltonian

$$H_{\text{eff}} = \frac{\alpha\Omega}{2} |\Psi_s\rangle \langle \uparrow\uparrow\uparrow | + h.c, \quad (3)$$

in which  $\alpha$  is character parameter which is determined by its configuration. Transforming back to the lab frame, the time evolution of the initial state  $|\Psi_1\rangle$  may be written as

$$|\uparrow\uparrow\uparrow\rangle \rightarrow \cos[\theta(t)] |\uparrow\uparrow\uparrow\rangle + e^{-i\omega_l t} \sin[\theta(t)] |\Psi_s\rangle \quad (4)$$

where  $\theta(t) = \frac{\alpha}{2} \int dt \Omega$ . In this way, through the resonant interaction Eq.(3), one can choose the interaction time  $t$  with  $\theta(t) = \pi$ , the state  $|\uparrow\uparrow\uparrow\rangle$  will acquire an  $e^{i\pi}$  phase factor, i.e.,

$$|\uparrow\uparrow\uparrow\rangle \rightarrow -|\uparrow\uparrow\uparrow\rangle \quad (5)$$

The polarized laser field can not induce transitions through initial states to exciton states in any other subspaces. The state  $|\downarrow\downarrow\downarrow\rangle$  can not evolve under  $\sigma^+$  polarized light for the Pauli blocking principle. And electronic states owing single  $|\uparrow\rangle$  and that owing double  $|\uparrow\rangle$  are off-resonant with their single-exciton states via the large detuning  $\Delta$ , which is tuned large enough such that  $\Delta \gg \Omega$ . Therefore, the classical light field combing the coupling between the dots can create a  $\pi$  phase shift on the state  $|\downarrow\downarrow\downarrow\rangle$  and leave the other seven electronic state unevolved, implementing the three-qubit CPHASE gate.

*Dephasing due to the phonon bath.*—In the actually phase gate, the coupling with the phonon bath can lead to dephasing, which degrade the quality of the phase gate. We focus on the low temperature regime, hence only the acoustic phonons will contribute to the dephasing process[16, 17]. The exciton phonon interaction can be described by

$$H_{ep} = \sum_{j=1}^3 \sum_{\mathbf{q}} g_{q,j} c_j^\dagger c_j (a_{\mathbf{q}} + a_{\mathbf{q}}^\dagger) \quad (6)$$

with the effective excitonic coupling strength

$$g_{\mathbf{q},j} = \sum_{\mathbf{q}} e^{i\mathbf{q}\cdot\mathbf{d}_j} [M_{q,j}^e \rho_e(\mathbf{q}) - M_{q,j}^h \rho_h(\mathbf{q})], \quad (7)$$

where  $M_{q,j}^{e/h} = \sum_{\mathbf{q}} \sqrt{\hbar|q|/2\mu V c_s} D_{e/h}$ , and the state density in  $\mathbf{k}$  space  $\rho_{e/h}(\mathbf{q}) = \int d^3r |\phi_{e/h}|^2 e^{i\mathbf{q}\cdot\mathbf{r}}$ .  $a_{\mathbf{q}}(a_{\mathbf{q}}^\dagger)$  are the annihilation(creation) operators for phonons with wave vector  $\mathbf{q}$ ,  $\mu$  denotes the mass density,  $V$  is the normalization volume, and  $D_{e(h)}$  is the deformation potential coupling constant of elector (hole). The wave function we choose

is  $\phi_{e/h} \sim \exp(-r^2/l_{e/h}^2)$  with the electron(hole) ground-state localization length. Because the wave function has spherical symmetry, only the longitudinal acoustic phonon (LA) will contribute to the decoherence process. Under the Markovian approximation, the master equation of the density for the whole system can be read as in a Lindblad form[9]

$$\begin{aligned} \dot{\rho} = & -i[H_s, \rho] + \mathcal{R}[\rho] + \sum_i J(\omega_i)([N(\omega_i) + 1]D[L_i]\rho \\ & + N(\omega_i)D[L_i^\dagger]\rho). \end{aligned} \quad (8)$$

with  $H_s = H_0 + H_i$ , and  $\mathcal{R}[\rho] = \sum_{i=1}^3 \Gamma[\sigma_{i-}\rho\sigma_{i+} - \frac{1}{2}(\sigma_{i+}\sigma_{i-}\rho + \rho\sigma_{i+}\sigma_{i-})]$  depicting the photon emission effect and  $\sigma_{i-} = |\uparrow\rangle_i\langle X_{\uparrow}^+|$  (or  $\sigma_{i+} = |X_{\uparrow}^+\rangle_i\langle\uparrow|$ ) denoting the lowering (or raising) operators of  $i^{th}$  dot.  $\Gamma$  is the spontaneous radiative decay rate, which is inversely proportional to the lifetime of exciton.  $D[L]\rho = L\rho L^\dagger - \frac{1}{2}(L^\dagger L\rho + \rho L^\dagger L)$  is the decay operator of phonon effect, and  $N(\omega) = [\exp(\omega/k_B T) - 1]^{-1}$  is the thermal occupation of the phonon modes.  $J(\omega_i)$  is the phonon spectral density, which is determined by the configuration. Here we mainly focus on the widely studied InAs/GaAs QDs, and we choose the parameter  $V_F = 0.85$  meV, Exciton energy  $\omega_a = 1.1$  eV, bi-exciton binding energy  $V_{xx} = 5$  meV, radiative decay rate  $\Gamma = 1.6 \mu$  eV, electron and hole ground state localization length  $l_e = 2.16$  nm,  $l_h = 1.44$  nm, mass density  $\mu = 5.3\text{k/cm}^3$  and the sound velocity  $c_s = 4.8 \times 10^5$  cm/s.

In the following, we will study two schemes for the phases gate according to the different configurations of three QDs.

*Ring configuration.* – In the ring-arrayed QDs, we first reduce the Hamiltonian Eq.(1) into the subspace  $\mathcal{H}$ . When  $\Omega = 0$ , the eigenstates of  $\mathcal{H}$  are  $|\Psi_1\rangle = |\uparrow\uparrow\uparrow\rangle$ ,  $|\Psi_2^*\rangle = \frac{1}{\sqrt{6}}(c_1^\dagger - 2c_2^\dagger + c_3^\dagger)|\uparrow\uparrow\uparrow\rangle$ ,  $|\Psi_3^*\rangle = -\frac{\sqrt{2}}{2}(c_1^\dagger - c_3^\dagger)|\uparrow\uparrow\uparrow\rangle$ ,  $|\Psi_4\rangle = \frac{1}{\sqrt{3}}(c_1^\dagger + c_2^\dagger + c_3^\dagger)|\uparrow\uparrow\uparrow\rangle$ . Considering the case  $\Omega \ll V_F \ll V_{xx}$ , double and ternate trion states are adiabatically eliminated.

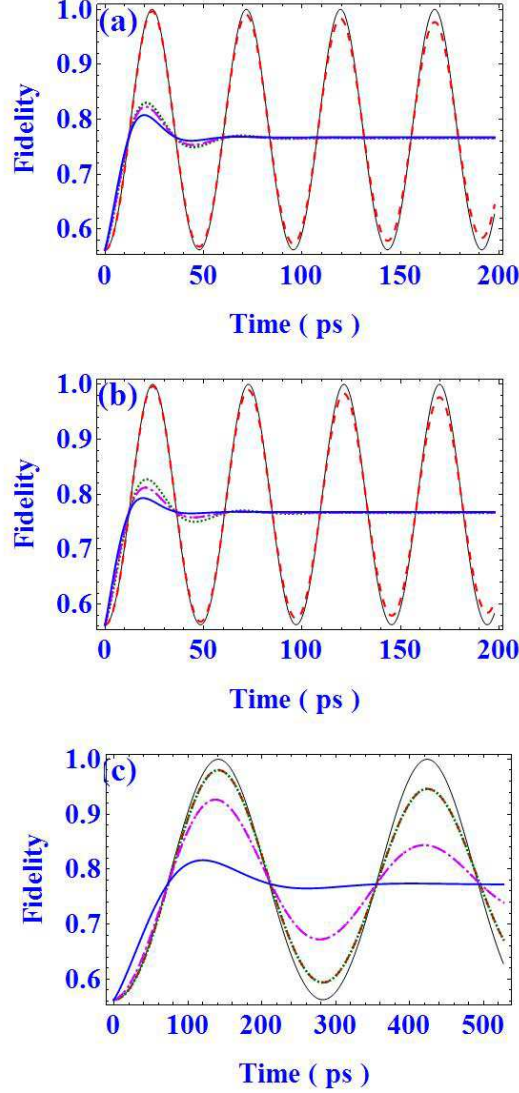


FIG. 2: (color online). The fidelity of the CPHASE gate in three cases against delay time(ps) with  $\Omega = 0.1$  meV and  $2R = 6$  nm : (a) for ring configuration, (b) for line configuration with transition  $|\Psi_1\rangle \leftrightarrow |\Psi_4\rangle$ , (c) for line configuration with transition  $|\Psi_1\rangle \leftrightarrow |\Psi_2\rangle$ . We present five curves in each figure to describe performance of CPHASE gate operation in different conditions: without noise(black, solid line), only spontaneous radiation(red, dashed line), combing both spontaneous and phonon effect at three finite temperature, respectively. In (a) and (b), temperature  $T$  varies from  $T = 0K$ (green, dotted line),  $10K$ (Pink, dash-dot line),  $20K$ (blue, solid line). While,  $T$  are chosen to be  $0K$ (green, dotted line),  $5K$ (Pink, dash-dot line),  $10K$ (blue, solid line) in (c).

Moreover, the anti-symmetry basis  $|\Psi_2^*\rangle, |\Psi_3^*\rangle$  have no effect on the initial state  $|\Psi_1\rangle$ , so we could only choose the higher single-exciton state  $|\Psi_4\rangle$  as an auxiliary state  $|\Psi_s\rangle$ , and set  $\omega_l = \omega_a + 2V_F$ . It can be obtained that  $\alpha_{ring} = \sqrt{3}$ , and the effective Hamiltonian in ring-structure is  $H_{\text{eff}} = \frac{\sqrt{3}\Omega}{2}|\Psi_4\rangle\langle\Psi_1| + h.c.$

In Fig. 2, we present the fidelity of the CPHASE gate with  $\Omega = 0.1$  meV and  $2R = 6$  nm, where the input state is  $|\Psi_i\rangle = [\frac{1}{\sqrt{2}}(|\uparrow\rangle + |\downarrow\rangle)]^{\otimes 3}$ , and the ideal state is  $|\Psi_f\rangle = \frac{1}{2\sqrt{2}}(|\downarrow\downarrow\downarrow\rangle + |\uparrow\downarrow\downarrow\rangle + |\downarrow\uparrow\downarrow\rangle + |\downarrow\downarrow\uparrow\rangle + |\uparrow\uparrow\downarrow\rangle + |\uparrow\downarrow\uparrow\rangle + |\downarrow\uparrow\uparrow\rangle - |\uparrow\uparrow\uparrow\rangle)$  after the gate operation. The fidelity here is defined as  $\mathcal{F} = |\langle\Psi_f|\rho|\Psi_f\rangle|$ . The black solid line is the result that set  $\Gamma = 0$ , which shows perfect Rabi oscillation. Then we consider the phonon effect. We have demonstrated that the single-exciton state  $|\Psi_2^*\rangle$  and  $|\Psi_3^*\rangle$  are decoupled from the evolution of  $H_{\text{sub}}$  in the case without environment fluctuation. However,  $|\Psi_2^*\rangle$  and  $|\Psi_3^*\rangle$  are degenerated with energy lower than  $|\Psi_4\rangle$ , so spontaneous photon emission and phonon interaction lead to an intense dissipation and  $|\Psi_2^*\rangle$  and  $|\Psi_3^*\rangle$  should be reconsidered in our model. The new Hamiltonian is  $H = H'_{\text{sub}} + \sum_{\mathbf{q}} \omega_q(a_{\mathbf{q}}^\dagger a_{\mathbf{q}}) + H_{ep}$ , where  $H'_{\text{sub}} = -V_F|\Psi_2^*\rangle\langle\Psi_2^*| - V_F|\Psi_3^*\rangle\langle\Psi_3^*| + \frac{\sqrt{3}\Omega}{2}(|\Psi_1\rangle\langle\Psi_4| + h.c.)$ . In the basis consisted by the eigenstates of  $H'_{\text{sub}}$  ( $|\Phi_1\rangle = \frac{1}{\sqrt{2}}(|\Psi_1\rangle - |\Psi_4\rangle)$ ,  $|\Phi_2\rangle = |\Psi_2^*\rangle$ ,  $|\Phi_3\rangle = |\Psi_3^*\rangle$ ,  $|\Phi_4\rangle = \frac{1}{\sqrt{2}}(|\Psi_1\rangle + |\Psi_4\rangle)$ ), we move the Hamiltonian into an interaction picture with respect to  $H'_{\text{sub}} + \sum_{\mathbf{q}} \omega_q(a_{\mathbf{q}} a_{\mathbf{q}}^\dagger)$ , and calculate the density operator by approaches mentioned above. The distance between the center of the ring configuration and each dot is  $d = \sqrt{3}$  nm. We set the coordinates of three dots to be  $(-\frac{d}{2}, -\frac{\sqrt{3}d}{2}, 0)$ ,  $(d, 0, 0)$  and  $(-\frac{d}{2}, \frac{\sqrt{3}d}{2}, 0)$ . The spectral densities  $J(\omega)$  with their relevant parameters shown in Table. I.

In order to validate the performance of the proposed phase gate, we perform a direct numerical simulation with the full master equation Eq. (8). In Fig. 2, it is shown that the Rabi oscillations in fidelity are quickly damped primarily due to phonon-exciton interaction,

$J(\omega)$	$L$	$\omega$
$8\pi\mathbb{G}(\omega)[1 - \frac{\sin(\sqrt{3} \mathbf{q} d)}{\sqrt{3} \mathbf{q} d}]$	$\frac{1}{2\sqrt{3}} \Phi_2\rangle\langle\Phi_4 $	$3V_F + \frac{1}{2}\alpha\Omega$
	$\frac{1}{2\sqrt{3}} \Phi_2\rangle\langle\Phi_1 $	$3V_F - \frac{1}{2}\alpha\Omega$
$3\pi\mathbb{G}(\omega)( \mathbf{q} d)^2[4 - \frac{3}{5}( \mathbf{q} d)^2]$	$\frac{1}{6} \Phi_3\rangle\langle\Phi_4 $	$3V_F + \frac{1}{2}\alpha\Omega$
	$\frac{1}{6} \Phi_3\rangle\langle\Phi_1 $	$3V_F - \frac{1}{2}\alpha\Omega$
$3\pi\mathbb{G}(\omega)[12 - 4( \mathbf{q} d)^2 + \frac{3}{5}( \mathbf{q} d)^4]$	$\frac{1}{6} \Phi_1\rangle\langle\Phi_4 $	$\alpha\Omega$

TABLE I: Calculation results of spectral densities with different frequencies and dissipative operators in ring configuration. Here  $\mathbb{G}(\omega) = \frac{\omega^3}{8\pi^2\mu c_s^3}[D_e \exp(-(\frac{\omega d_e}{2c_s})^2) - D_h \exp(-(\frac{\omega d_h}{2c_s})^2)]^2$  is the common factor of all spectral densities in ring structure,  $\alpha_{ring} = \sqrt{3}$  is the character factor in ring configuration and  $|\mathbf{q}| = \omega/c_s$ .

and no clear oscillation period is observable even if temperature achieved at its limit 0K. As temperature  $T$  increases, the system suffers a stronger damping. The spontaneous radiation is also a decoherent source of damping, but the influence is so small that Rabi oscillations are obvious in a relatively long timescale.

*Line Configuration.*— The analysis of the line configuration can be derived in analog to the ring-configuration. In subspace  $\mathcal{H}$ , eigenstates for  $\Omega = 0$  include  $|\Psi_1\rangle = |\uparrow\uparrow\uparrow\rangle$ ,  $|\Psi_2\rangle = \frac{1}{2}(c_1^\dagger - \sqrt{2}c_2^\dagger + c_3^\dagger)|\uparrow\uparrow\uparrow\rangle$ ,  $|\Psi_3^*\rangle = -\frac{\sqrt{2}}{2}(c_1^\dagger - c_3^\dagger)|\uparrow\uparrow\uparrow\rangle$ , and  $|\Psi_4\rangle = \frac{1}{2}(c_1^\dagger + \sqrt{2}c_2^\dagger + c_3^\dagger)|\uparrow\uparrow\uparrow\rangle$ . The energy level diagram is illustrated in Fig.1(d). It is shown that both  $|\Psi_2\rangle$  and  $|\Psi_4\rangle$  have an energy shift comparing with other single exciton state, and can be chosen as auxiliary level resonated with  $|\Psi_1\rangle$  to prepare a CPHASE Gate.

If we pump the laser with frequency  $\omega_l = \omega_a - \sqrt{2}V_F$ , the transition  $|\Psi_1\rangle \leftrightarrow |\Psi_2\rangle$  is allowed (in Fig. 1). We can obtain the character factor of configuration  $\alpha_{down} = 1 - \frac{\sqrt{2}}{2}$ ,  $H_{eff}(t) = \frac{\Omega}{2}(1 - \frac{\sqrt{2}}{2})(|\Psi_1\rangle\langle\Psi_2| + H.c.)$ . In the case of  $\int_0^{t_I} \frac{\Omega}{2}(1 - \frac{\sqrt{2}}{2})dt = \pi$ , a  $\pi$ -pulse shift

$J(\omega)$	$L_{down}$	$L_{up}$	$\omega$
$2 \sin( \mathbf{q} d)\mathbb{G}(\omega)$	$\frac{1}{4} \Phi_1\rangle\langle\Phi_3 $	$\frac{1}{2\sqrt{2}} \Phi_2\rangle\langle\Phi_3 $	$\sqrt{2}V_F + \frac{1}{2}\alpha\Omega$
	$\frac{1}{4} \Phi_2\rangle\langle\Phi_3 $	$\frac{1}{4} \Phi_3\rangle\langle\Phi_4 $	$\sqrt{2}V_F$
	$\frac{1}{2\sqrt{2}} \Phi_3\rangle\langle\Phi_4 $	$\frac{1}{4} \Phi_3\rangle\langle\Phi_1 $	$\sqrt{2}V_F - \frac{1}{2}\alpha\Omega$
$4 \sin^2(\frac{ \mathbf{q} d}{2})\mathbb{G}(\omega)$	$\frac{1}{4\sqrt{2}} \Phi_1\rangle\langle\Phi_4 $	$\frac{1}{4\sqrt{2}} \Phi_2\rangle\langle\Phi_4 $	$2\sqrt{2}V_F + \frac{1}{2}\alpha\Omega$
	$\frac{1}{4\sqrt{2}} \Phi_2\rangle\langle\Phi_4 $	$\frac{1}{4\sqrt{2}} \Phi_2\rangle\langle\Phi_1 $	$2\sqrt{2}V_F - \frac{1}{2}\alpha\Omega$
$4 \cos^2(\frac{ \mathbf{q} d}{2})\mathbb{G}(\omega)$	$\frac{1}{8} \Phi_1\rangle\langle\Phi_2 $	$\frac{1}{8} \Phi_1\rangle\langle\Phi_4 $	$\alpha\Omega$

TABLE II: Calculation results of spectral densities with different frequencies and dissipative operators in line configuration. Here  $\mathbb{G}(\omega) = \frac{\omega^3}{2\pi\mu c_s^3} [D_e \exp(-(\frac{\omega d_e}{2c_s})^2) - D_h \exp(-(\frac{\omega d_h}{2c_s})^2)]^2$  is the common factor of all spectral densities in line structure, and  $|\mathbf{q}| = \omega/c_s$ . The character factor  $\alpha$  has two different value when choosing different resonant transitions in the line configuration. If resonant transition is selected as  $|\Psi_1\rangle \leftrightarrow |\Psi_2\rangle$ ,  $\alpha$  becomes as  $\alpha_{down} = 1 - \frac{\sqrt{2}}{2}$ , and relative decay operator is  $L_{down}$ ; while  $\alpha$  becomes as  $\alpha_{up} = 1 + \frac{\sqrt{2}}{2}$ , and decay operator is  $L_{up}$  if  $|\Psi_1\rangle \leftrightarrow |\Psi_4\rangle$  is selected.

on the system engenders:  $|\uparrow\uparrow\uparrow\rangle \rightarrow -|\uparrow\uparrow\uparrow\rangle$ .

If we let the laser be resonant with transition  $|\Psi_1\rangle \leftrightarrow |\Psi_4\rangle$  (simply replace  $\omega_l$  by  $\omega_l = \omega_a + \sqrt{2}V_F$ ), the factor  $\alpha$  becomes as  $\alpha_{up} = 1 + \frac{\sqrt{2}}{2}$ , a similar Hamiltonian is  $H_{eff}(t) = \frac{\Omega}{2}(1 + \frac{\sqrt{2}}{2})(|\Psi_1\rangle\langle\Psi_2| + H.c.)$ , and the  $\pi$ -pulse shift may occur when  $\int_0^{t_I} \frac{\Omega}{2}(1 + \frac{\sqrt{2}}{2})dt = \pi$  and the operation time could be obviously shortened.

Like the ring configuration, we can also derive a new density operator to describe the evolution of line configuration. The distance between the center of the ring configuration and each dot is  $2d = 6$  nm. Here the coordinates of three dots are chosen as  $(-d, 0, 0)$ ,  $(0, 0, 0)$  and  $(d, 0, 0)$ , then we can obtain spectral densities  $J(\omega)$ (listed in Table. II) in two strategies about the selection of resonant transition from ground state to  $|\Psi_2\rangle$  (*low-level*) or high

exciton energy level  $|\Psi_4\rangle$ (*high-level*) , and then we may find that two numerical calculation results in the same configuration is totally different. In Fig. 2, it is demonstrated that, in the *low-level* case, phonon effect does not lead a strong damping at very low temperature. Especially at 0K, the behavior is as the same as that only considering spontaneous radiation. This is because spectral density  $J(\omega)$  between ground state and low single exciton level is close to zero. As the temperature is increased, oscillations are damped: for  $T = 5\text{K}$ , two periods of oscillation are still visible, while no clear oscillation is exhibited for  $T = 10\text{K}$ . In the *high-level* case, like the ring configuration, phonon effect plays a dominant role in decoherence mechanism. Moreover, the damping induced by phonon effect is a little larger than ring configuration at the same temperature.

*Conclusion.*—In this work, we discuss the configuration effect and acoustic phonon effect on the CPHASE gate. We found that the quality of the phase gate depends strongly on the configuration, which is of great importance when QDs is used as building block to larger integrated systems. We also found that those configuration mainly influence the energy levels, hence influence the exciton phonon coupling strength. We show that the line configuration with resonant transition  $|\Psi_1\rangle \leftrightarrow |\Psi_2\rangle$  is more suitable for quantum computation.

S. Y would like to thank Dr. Erik. M. Gauger for his kind and warm help by Email. This work was supported by National Fundamental Research Program, also by National Natural Science Foundation of China (Grant No. 10674128 and 60121503) and the Innovation Funds and “Hundreds of Talents” program of Chinese Academy of Sciences and Doctor Foundation of Education Ministry of China (Grant No. 20060358043).

---

[1] Q. A. Turchette, C. J. Hood, W. Lange *et al*, *Phy. Rev. Lett.* **75**, 4710 (1995).

- [2] C. Monroe, D. M. Meekhof *et al*, *Phy. Rev. Lett.* **75**, 4714 (1995).
- [3] J. A. Jones *et al*, *Nature (London)*, **393**, 344 (1998).
- [4] X. Li, Y. Wu *et al*, *Science* **301**, 809 (2004).
- [5] Y. Yamamoto *et al*, *Nature (London)* **425**, 941 (2004).
- [6] C. H. van der Wals, A. C. J. ter Harr *et al*, *Science*, **290**, 773 (2000).
- [7] A. Imamoglu, D.D. Awschalom, G. Burkard, D. P. DiVincenzo, D. Loss, M. Sherwin, and A. Small, *Phys. Rev. Lett.* **83**, 4204 (1999).
- [8] S. Cortez, O. Krebs, S. Laurent, M. Senes, X. Marie, P. Voisin, R. Ferreira, G. Bastard, J-M. Gerard, and T. Amand, *Phys. Rev. Lett.* **89**, 207401 (2002).
- [9] Erik M.Gauger, Simon C. Benjamin, Absan Nazir, and Brendon W. Lovett, *Phys. Rev. B* **77**, 115322 (2008).
- [10] Erik M.Gauger, Absan Nazir, Simon C. Benjamin, Thomas M Stace, and Brendon W. Lovett, [arXiv:0804.2139v1](https://arxiv.org/abs/0804.2139v1).
- [11] P. Borri, W. Langbein, S. Schneider, U. Woggon, R. L. Sellin, D. Ouyuan, and D. Bimberg, *Phys. Rev. Lett.* **87**, 157401 (2001).
- [12] DaeGwi Kim, Shinya Okahara, Masaaki Nakayama and YongGu Kim, *Phys. Rev. B* **78**, 153301 (2008).
- [13] Yoshiaki Rikitake and Hiroshi Imamura, *Phys. Rev. B* **74**, 081307(R) (2006).
- [14] Z. Diao, M. S. Zubairy, and G. Chen, *Z. Naturforsch., A: Phys. Sci.* **57**, 701 (2002).
- [15] D. Jaksch, J. I. Cirac, P. Zoller, S. L. Rolston, R.Côté, and M.D.Lukin, *Phys. Rev. Lett.* **85**, 2208 (2000).
- [16] W. Ben Chouikha, S. Jaziri, and R. Bennaceur, *Physica E*, **39**, 15 (2007).
- [17] B. Krummheuer, V. M. Axt, and T. Kuhn, *Phys. Rev. B*, **65**, 195313 (2002).